

Volume 32, Number 3, June 2006

The bidirectional reflectance distribution function (BRDF) of a moss canopy (*Pleurozium schreberi*) measured by the University of Lethbridge Goniometer System. For further information, see Coburn and Peddle, pp. 244–253.

La fonction de distribution de la réflectance bidirectionnelle (FDRB) d'un couvert de mousse (*Pleurozium schreberi*) mesurée à l'aide du système de goniomètre de l'Université de Lethbridge. Pour plus d'information, consulter Coburn et Peddle, p. 244–253.

Table of Contents

Volume 32, Number 3, June 2006

E-ISSN [1712-7971](https://doi.org/10.1080/1712-7971)

[Full Issue in PDF / Numéro complet en PDF](#)

[Earth observation data and geographical information system \(GIS\) techniques for earthquake risk assessment in the western Gulf of Corinth, Greece](#)

Is. Parcharidis, C. Metaxas, and E. Vassilakis

Pages 223-227

[Abstract](#)

[Linking riparian vegetation spatial structure in Australian tropical savannas to ecosystem health indicators: semi-variogram analysis of high spatial resolution satellite imagery](#)

Kasper Johansen and Stuart Phinn

Pages 228-243

[Abstract](#)

[A low-cost field and laboratory goniometer system for estimating hyperspectral bidirectional reflectance](#)

C.A. Coburn and D.R. Peddle

Pages 244-253

[Abstract](#)

[Investigation of the MODIS snow mapping algorithm during snowmelt in the northern boreal forest of Canada](#)

S.K.M. Poon and C. Valeo

Pages 254-267

[Abstract](#)

Research Note / Note de recherche

Earth observation data and geographical information system (GIS) techniques for earthquake risk assessment in the western Gulf of Corinth, Greece

Is. Parcharidis, C. Metaxas, and E. Vassilakis

Abstract. This study attempts to demonstrate the utility of differential synthetic aperture radar (SAR) interferometry and very high resolution satellite optical data for the assessment of earthquake risk, using a geographical information system (GIS), in the western part of the Gulf of Corinth, a seismically active region of Greece that suffered the effects of the Eigion earthquake (magnitude $M = 6.1$) of 15 June 1995. During the project, both archive and newly acquired European remote sensing satellite (ERS) data were used to generate conventional differential interferograms and produce a deformation map over the area. An IKONOS-2 image was used to create and update information concerning urban structures like buildings, road networks, and facilities like hospitals, churches, and factories. A first attempt to evaluate the Earth observation (EO) contribution in the earthquake risk assessment system shows that the differential interferometric synthetic aperture radar (DInSAR) is suitable only for co-seismic deformation monitoring, and very high resolution data perform very well in the mapping of urban structures.

Résumé. Cette étude vise à faire la démonstration de l'utilité de l'interférométrie différentielle radar à synthèse d'ouverture (RSO) et des données satellitaires optiques à très haute résolution pour l'évaluation du risque de séisme à l'aide d'un système d'information géographique (SIG) dans la partie ouest du golfe de Corinthe, une région de la Grèce active au plan séismique qui a subi les effets du séisme de Eigion ($M = 6,1$), en juin 1995. Au cours du projet, des données ERS (« European remote sensing satellite ») archivées de même que des données nouvellement acquises ont été utilisées pour générer des interférogrammes différentiels conventionnels et pour produire une carte des déformations de la zone. Une image IKONOS-2 a été utilisée pour créer et mettre à jour l'information se rapportant aux structures urbaines telles que les pâtés de maisons, le réseau routier, les équipements, etc. Un premier essai d'évaluation de la contribution des données d'OT dans le système d'évaluation du risque de séisme indique, d'une part, que le système DInSAR (« differential interferometric synthetic aperture radar ») est utile uniquement pour le suivi des déformations co-séismiques et, d'autre part, que les données à très haute résolution spatiale ont un niveau de performance élevé pour la cartographie des structures urbaines. [Traduit par la Rédaction]

Introduction

This paper describes the results of the E.C. project (short title "SNAP") concerning the demonstration of the utility of differential interferometric synthetic aperture radar (DInSAR) and high-resolution optical data for the assessment of earthquake risk in a seismically active region of Greece.

In mitigation, Earth observation (EO) is useful for base mapping for emergency relief logistics and the estimation of settlement and structure vulnerability (e.g., building design) and exposure. In the response phase, the improving contribution by EO in damage mapping is an issue of prime concern to relief agencies, which need to locate possible victims and structures at risk, and to the insurance industry, which needs to assess losses.

DInSAR is a technique that can be used for the detection of crustal deformation using suitable pairs of synthetic aperture radar (SAR) images. DInSAR can deliver spectacular measurements of the large-scale ground deformations

associated with main earthquake events (Massonnet et al., 1993; Zebker et al., 1994), provided the temporal separation and horizontal baseline between the two SAR images are kept within appropriate limits. Many examples exist, and such results on their own offer unique input to strain models, support the understanding of fault mechanisms, and have even been successfully used for the verification of insurance claims. Although usually applicable to the main co-seismic event, and hence perhaps a "response" technique, the deformation

Received 28 March 2005. Accepted 26 April 2006.

Is. Parcharidis.¹ Department of Geography, Harokopio University, El. Venizelou 70, 17672 Athens, Greece.

C. Metaxas. Earthquake Planning and Protection Organization, Xanthou 32, 15452, N. Psychiko, Athens, Greece.

E. Vassilakis. Department of Geology, University of Athens, Panepistimioupolis, Ilissia, 15784 Athens, Greece.

¹Corresponding author (e-mail: parchar@hua.gr).

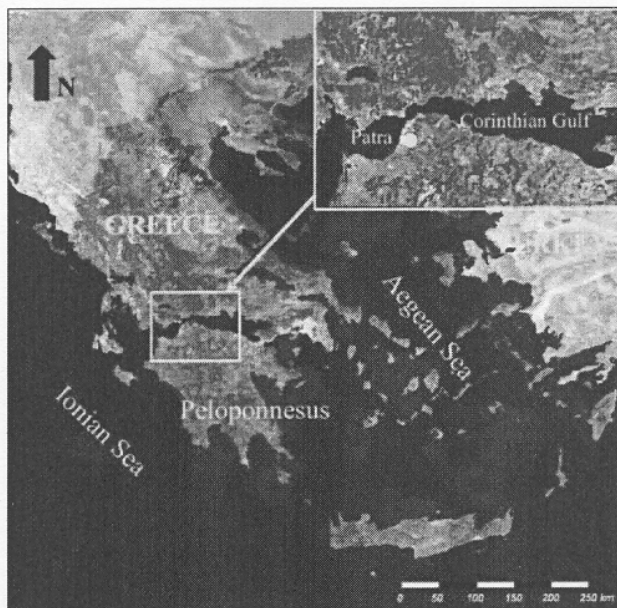


Figure 1. Satellite image of Greece showing the location of western Corinthian Gulf (medium-resolution imaging spectroradiometer (MERIS) image from the European Space Agency).

information can provide valuable understanding of fault mechanisms and thus input to forecast models in the mitigation phase. The displacement resolution of the technique is degraded by parameters such as (i) loss of coherence, (ii) atmospheric artifacts, (iii) uncompensated topography, and (iv) instrumental limitations (Zebker and Villasenor, 1992; Goldstein, 1995).

Description of the study area

The Gulf of Corinth is located in central Greece and separates the Peloponnese from the mainland of Greece (Figure 1). During the last decade, this area has been affected by two destructive earthquakes, one on 14 July 1993 (magnitude $M = 5.4$) and one on 15 June 1995 ($M = 6.1$). There has been a significant amount of geological and seismological interest in the area by a large number of researchers (for example, Tselentis and Makropoulos, 1986; Doutsos et al., 1988; Billiris et al., 1991; Armijo et al., 1996; Rigo et al., 1996; Bernard et al., 1997; Briole et al., 2000; Sorel, 2000; Morewood and Roberts, 2001).

Patra is the largest city in the study area and one of the most important economic and administrative centres of western Greece. The social infrastructure of Patra is of great importance for a much broader area, and the city is a large transportation centre that is likely to develop as such after the construction of

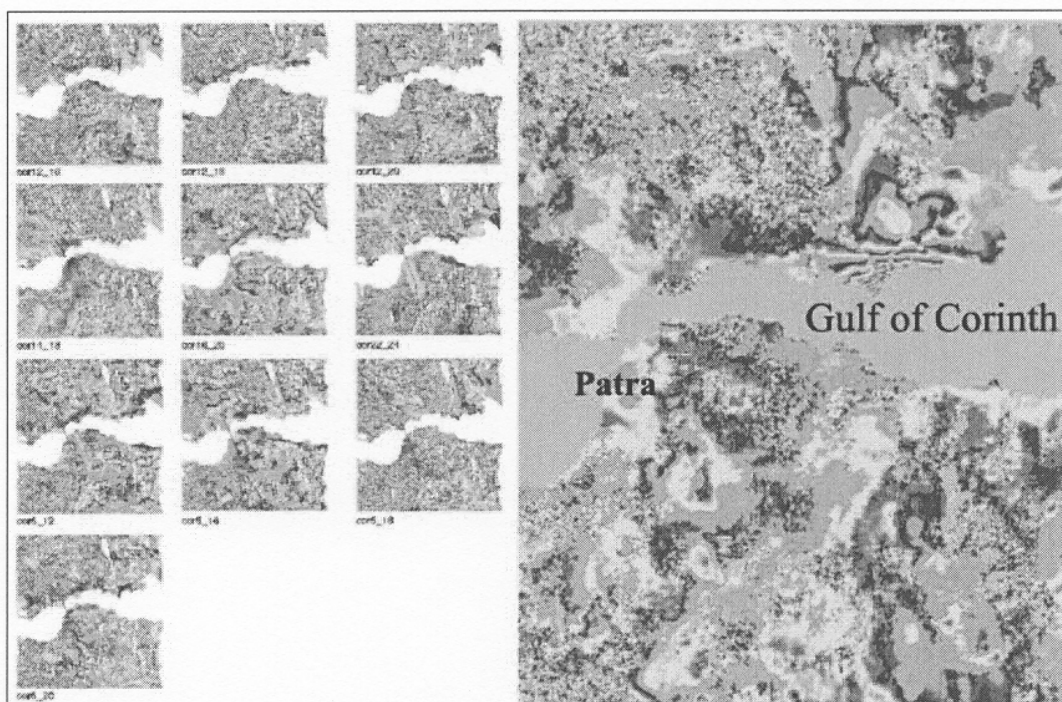


Figure 2. Inter-seismic interferograms in the western Gulf of Corinth and Patra area and the differential interferogram produced of the Aigion earthquake that occurred on 15 June 1995. In the northern coastal zone, the fringes representing the associated deformation are clearly visible. Every cycle of red–green–blue (RGB) colors corresponds to 28 mm of deformation along the line of sight of the radar beam.

new infrastructure projects of national and European importance such as the Rio-Antirio Bridge and the new port of Patra.

SAR and optical data collection and processing

SAR data and processing

The initial conventional InSAR processing strategy was to process inter-Bperp (Bperp is a component of the baseline perpendicular to the SAR slant range direction) compliant SAR data pairs for 4-month periods spanning the European remote sensing satellite (ERS) archive. This strategy, however, relied on the availability of sufficient data with very tight (<50 m) Bperp ranges. In reality, the number of scenes available fell short of the ideal, and Bperps were thus quite variable. This strategy made the solution of atmospheric ambiguities difficult because of the use of common scenes that had been specifically chosen to form a data chain spanning the archive. Hence, 1-year independent pairs with a temporal overlap were used so that similar periods were covered by atmospheric-independent data. In total, 10 interferograms were generated (Figure 2). The coherence image was visually improved in each image pair after filtering, but remained low in many cases. As expected, regions with little vegetation, such as that near the Itea Peninsula in the northeast, were more coherent than the largely agricultural regions to the southwest of the images.

Tight fringe patterns occurred in the northeast corner of most interferograms and followed the major valleys in the region. It is unclear whether the observed fringes (corresponding to a ground displacement) are tectonically induced or whether there are atmospheric effects that occur systematically in each interferogram, e.g., due to topography. There is a distinct correlation between topography and variation in phase, however. The differential interferogram of the Eigion earthquake (Figure 2) that occurred on 15 June 1995 ($M = 6.1$) shows eight fringes in the northern coast of the Gulf of Corinth corresponding to 22 cm of ground deformation (each fringe corresponds to 28 mm of deformation along the line of sight).

Optical data

A very high resolution IKONOS-2 image was used to incorporate information concerning urban structure, such as buildings, road network, and facilities like hospitals, churches, and factories. Additional datasets were incorporated in the GIS, such as land cover classification using Landsat thematic mapper (TM) data, computed using an iterative mixture of spectral and manual classification techniques and seismically triggered landslide risk assessment, representing a significant risk to people living in earthquake-prone regions. A simplified Newmark method was used to model the seismically triggered landslide risk.

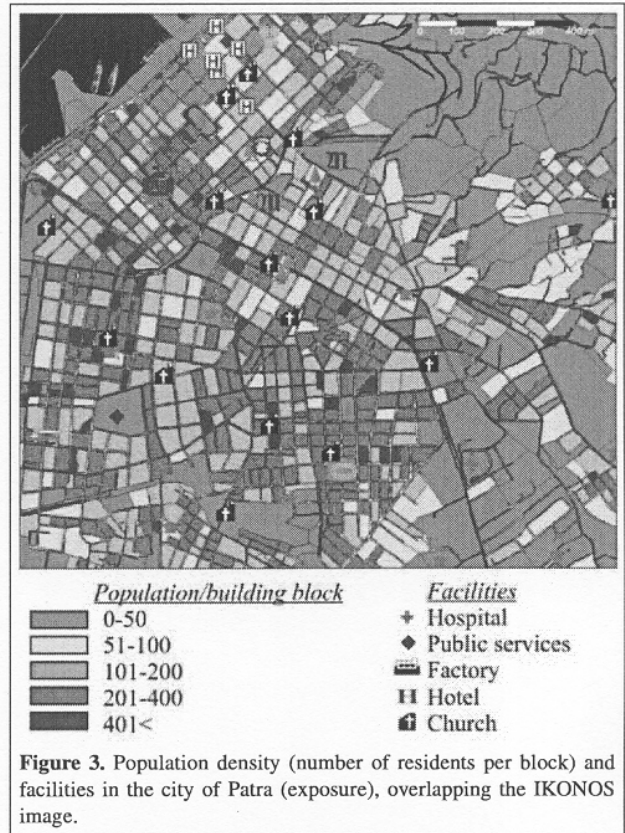
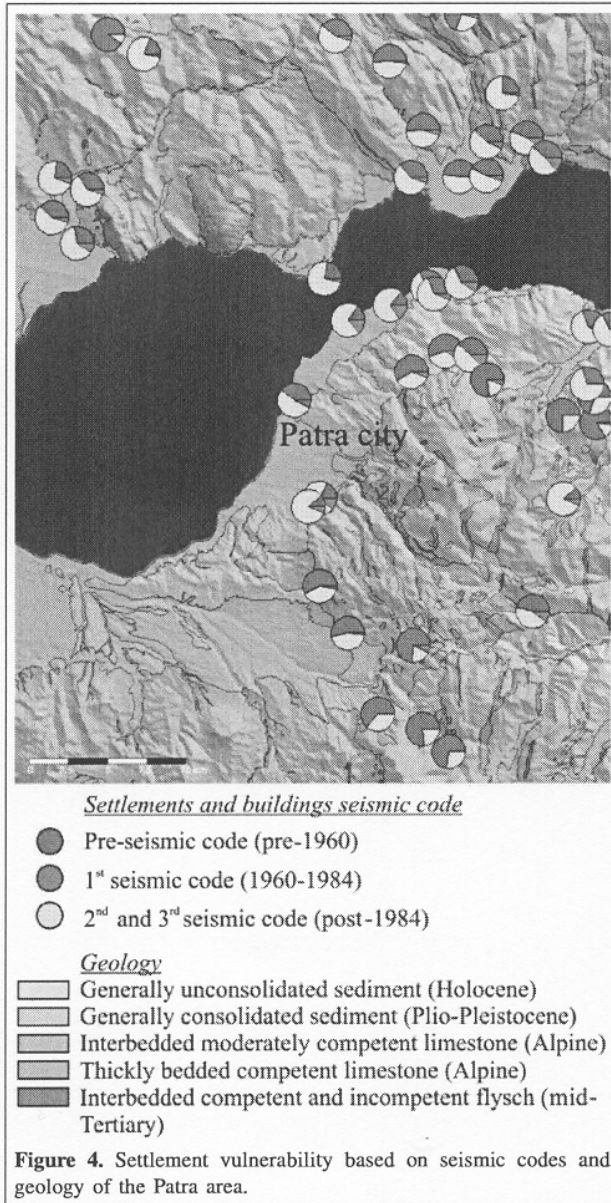


Figure 3. Population density (number of residents per block) and facilities in the city of Patra (exposure), overlapping the IKONOS image.

Seismic risk management system development

A GIS database was assembled to support the project and develop an earthquake risk management system. This system spatially coincides with the elements of the overall earthquake risk, which consists of the hazard (geophysical parameters), exposure (population and development), and vulnerability (ability of population and development to withstand the hazard). In particular, this system could demonstrate a way to a better understanding of the geospatial parameters in the preparedness and mitigation phases of an earthquake disaster. The GIS contained information at two scales, namely regional and detailed, around the city of Patra on the southern coast of the Gulf of Corinth. The different layers contained within the GIS include seismic hazard maps, earthquake epicentres, seismically triggered landslide hazard (hazard), population density, critical facilities, other facilities, transportation (exposure) and land cover classification, building age and construction material of settlements, and sensitive structures (vulnerability) (Figure 3).

The GIS formed the basic repository for the large amount of spatial data collected during the project and was developed into an earthquake risk management system in that it allowed the integration of various hazard, exposure, and vulnerability data



layers to generate new maps representing different aspects of earthquake risk (Figure 4).

Conclusions and discussion

The application of DInSAR in this study was aimed at the measurement of co-seismic and inter-seismic activity because the results can be of great benefit in the assembly of a GIS. By integrating these data with other relevant spatial data, an advanced tool useful for the assessment of damage and management of remediation can be constructed allowing priorities like mapping strategies by highlighting regions of

highest ground deformation. The major conclusions from the study are as follows:

- (1) Large-scale displacements associated with main earthquake events can be observed by conventional DInSAR. The results on their own offer unique input to strain models and support the understanding of fault mechanisms. DInSAR, however, is not considered a tool for the measurement of the millimetre-scale motions associated with annual inter-seismic activity, even given ideal data, which is a crucial parameter of seismic risk. The degraded resolution of conventional InSAR renders the technique more appropriate to larger scale displacements in terms of both magnitude and coverage, and thus it is more appropriate to the measurement of the main earthquake event. Given sufficient data (availability of SAR scenes), the millimetre accuracy of the permanent scatterers InSAR technique (Musson et al., 2004) could be an effective tool for the measurement of movement of the order of inter-seismic ground displacements.
- (2) Very high resolution EO data exhibit high performance either to update and refine existing data or to constitute the basic source of information for land use, land cover, and urban structure mapping. The use of these data requires powerful computing resources because of their large volume.

Acknowledgements

The authors wish to acknowledge Dr. Brian Damiata, Dr. Mark Haynes, and Dr. Ren Capes for providing valuable comments and suggestions.

References

Armijo, R., Meyer, B., King, G., and Papanastasiou, D. 1996. Quaternary evolution of the Corinth rift and its implications for the late Cenozoic evolution of the Aegean. *Geophysical Journal International*, Vol. 126, No. 1, pp. 11–53.

Bernard, P., Briole, P., Meyer, B., Lyon-Caen, H., Gomez, J.M., Tiberi, C., Berge, C., Cattin, R., Hatzfeld, D., Lachet, C., Lebrun, B., De-Schamps, A., Courboulex, F., Larroque, C., Rigo, A., Massonnet, D., Papadimitriou, P., Kassaras, J., Diagourtas, D., Makropoulos, K., Veis, G., Papazisi, E., Mitsakaki, C., Karakostas, V., Papadimitriou, E., Papanastasiou, D., Chouliaras, G., and Stavrakakis, G. 1997. The Ms = 6.2, June 15, 1995 Aigion earthquake (Greece): evidence for low angle normal faulting in the Corinth rift. *Journal of Seismology*, Vol. 1, pp. 131–150.

Billiris, H., Paradissis, D., Veis, G., England, P., Featherstone, W., Parsons, B., Cross, P., Rands, P., Rayson, P., Sellers, P., Ashkenazi, V., Davison, M., Jackson, J. and Ambraseys, N. 1991. Geodetic determination of tectonic deformations in Greece from 1900 to 1988. *Nature (London)*, Vol. 350, pp. 124–129.

Briole, P., Rigo, A., Lyon-Caen, H., Ruegg, J.C., Papazissi, K., Mitsakaki, C., Balodimou, A., Veis, G., Hatzfeld, D., and Deschamps, A. 2000. Active deformation of the Corinth rift, Greece: results from repeated Global Positioning System surveys between 1990 and 1995. *Journal of Geophysical Research*, Vol. 105, No. B11, pp. 25 605 – 25 626.

- Doutsos, T., Kontopoulos, N., and Poulimenos, G. 1988. The Corinth–Patras rift as the initial stage of continental fragmentation behind an active island arc (Greece). *Basin Research*, Vol. 1, pp. 177–190.
- Goldstein, R. 1995. Atmospheric limitations to repeat-track radar interferometry. *Geophysical Research Letters*, Vol. 22, pp. 2517–2520.
- Massonnet, D., Rossi, M., Carmona, C., Adragna, F., Peltzer, G., Feigl, K., and Rabauté, T. 1993. The displacement field of the Landers earthquake mapped by radar interferometry. *Nature (London)*, Vol. 364, pp. 138–142.
- Morewood, N.C., and Roberts, G.P. 2001. Comparison of surface slip and focal mechanism slip data along normal faults: an example from the eastern Gulf of Corinth, Greece. *Journal of Structural Geology*, Vol. 23, No. 2–3, pp. 473–487.
- Musson, R.M.W., Haynes, M., and Ferretti, A. 2004. Space-based tectonic modeling in subduction areas using PSInSAR. *Seismological Research Letters*, Vol. 75, No. 5, pp. 598–606.
- Rigo, A., Lyon-Caen, H., Armijo, R., Deschamps, A., Hatzfeld, D., Makropoulos, K., Papadimitriou, P., and Kassaras, I. 1996. A microseismic study in the western part of the Gulf of Corinth (Greece): implications for large-scale normal faulting mechanisms. *Geophysical International Journal*, Vol. 126, pp. 663–688.
- Sorel, D. 2000. A Pleistocene and still active detachment and the origin of the Corinth–Patras rift. *Geology*, Vol. 28, pp. 83–86.
- Tselentis, G., and Makropoulos, K. 1986. Rates of crustal deformation in the Gulf of Corinth (central Greece) as determined from seismicity. *Tectonophysics*, Vol. 124, pp. 55–66.
- Zebker, H., and Villasenor, J. 1992. Decorrelation in interferometric echoes. *IEEE Transactions in Geosciences and Remote Sensing*, Vol. 30, pp. 950–959.
- Zebker, H., Rosen, P., Goldstein, R., Gabriel, A., and Werner, C. 1994. On the derivation of coseismic displacement fields using differential radar interferometry: The Landers earthquake. *Journal of Geophysical Research*, Vol. 99, No. B10, pp. 19 617 – 19 634.